

Postfitting Control Scheme for Periodic Piezoscanner Driving

Shao-Kang HUNG^{1,3}, En-Te HWU^{2,3}, Ing-Shouh HWANG^{3*} and Li-Chen FU¹

¹Department of Electrical Engineering, National Taiwan University, Taipei 106, Taiwan, R.O.C.

²Department of Mechanical Engineering, National Taiwan University, Taipei 106, Taiwan, R.O.C.

³Institute of Physics, Academia Sinica, Taipei 115, Taiwan, R.O.C.

(Received July 4, 2005; revised September 18, 2005; accepted October 6, 2005; published online March 27, 2006)

The hysteresis and other nonlinear properties of piezoelectric scanners cause image distortion in scanning probe microscopy (SPM). Two types of control algorithm, feedback and feedforward, were applied to solve this problem. In general, a feedforward control method has a higher scanning speed, a higher resolution, but a lower accuracy than a feedback control method. In this paper, we propose a postfitting control scheme for driving the x -scanner of SPM periodically. This method possesses the advantages of both the feedback and feedforward methods, and achieves a higher image resolution and a higher accuracy than a pure feedback or feedforward method, without sacrificing scanning speed. [DOI: 10.1143/JJAP.45.1917]

KEYWORDS: scanning probe microscopy, piezoelectric nonlinearity, feedback control, feedforward control, hysteresis

1. Introduction

Piezoelectric scanners are widely used in scanning probe microscopy (SPM) because they have excellent resolution in displacement, high stiffness, and fast responses. A major drawback of piezoelectric materials, however, is its lack of accuracy due to many nonlinear characteristics, such as hysteresis,¹⁾ creep,¹⁾ and recoil-generated ringing,²⁾ which often cause distortion in SPM images. In general, the positioning error of a scanner caused by these nonlinearities may be as much as 10–15% of the full scanning range.³⁾ A physical explanation for hysteresis was given by Chen and Montgomery.⁴⁾ They proposed that hysteresis is a consequence of grain domain switching due to a change in the externally applied electric field. This domain switching occurs gradually. The lagging of the response might cause hysteresis and creep.

Many control schemes were proposed to deal with the positioning problems of piezoelectric actuators. They can be classified into two main categories: feedback (closed-loop) and feedforward (open-loop) methods. A feedback control system comprises a displacement sensor and a controller, which can be implemented using a digital computer or analog circuits. The controller tries to compensate the error between the desired trajectory and the measured displacement. From a simple proportional-integral-differential⁵⁾ (PID) algorithm to an advanced sliding-surface⁶⁾ scheme, many control schemes were proposed. For the feedforward methods, mathematical models of nonlinearities were proposed, such as the basic backlash model,⁷⁾ classical Preisach model,^{8–10)} generalized Maxwell Slip model,¹¹⁾ Bouc–Wen model,¹²⁾ and more complicated neural network model.^{13–15)} After performing specific identification experiments, modeling parameters can be obtained. Using effective models, one can build an estimator for predicting the motion and then preshape the driving signal in advance so that the positioning accuracy can be improved. This kind of method is also called the model-reference technique.¹⁶⁾ Another approach is to use a virtual, calculated inverse mathematical model^{17,18)} to cancel a physical plant. Figure 1 illustrates how the motion of a physical plant, a piezoelectric actuator, can follow the desired trajectory.

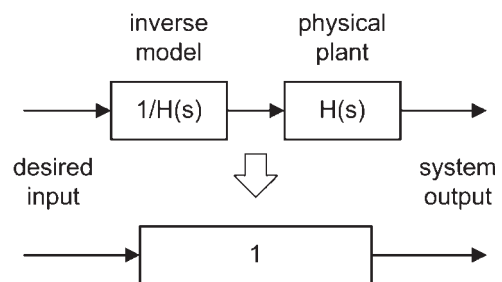


Fig. 1. Concept of inverse model compensation. $H(s)$ is a transfer function that represents the dynamics of a device, a piezoelectric actuator in the current case, we want to control. $H(s)$ can be obtained through a proper system identification experiment, and then $1/H(s)$ can also be derived. A fast digital signal processor (DSP) executing the calculation of $1/H(s)$ is placed in the front end of $H(s)$ to preshape the signal. Since the effects of $1/H(s)$ and $H(s)$ cancel out each other, the system output is thus equal to the desired input.

In the closed-loop approach, a high-gain¹⁹⁾ feedback control can be adopted to achieve a high scanning speed. However, the displacement measurement often has a high noise level when sensing a fast motion of a piezoelectric actuator, which results in a low spatial resolution in the driving signal. Generally, the resolution of a closed-loop system is tenfold lower than that of an open-loop system.²⁰⁾ A filter can be used to suppress the noise, but it also reduces scanning speed significantly. In contrast, feedforward control schemes can achieve a high scanning speed and a high resolution. Because no sensors are needed, the mechanical design of the system is much simpler and also more compact than that of the feedback control system. However, a major problem with feedforward control schemes is the time-varying characteristics of the piezoelectric materials. Although an accurate model can be found by appropriate identification tests at the beginning, the piezoelectric parameters of the scanner may vary with time due to the subsequent polarization/depolarization, pinning defects at grain boundaries, and warm-up. That is why feedforward control schemes usually suffer from poor accuracy and nonlinearity after some time. New identification tests have to be performed in order to maintain a certain accuracy.

Control algorithms combining both feedback and feedforward schemes have also been proposed,^{3,21,22)} unfortunately,

*Corresponding author. E-mail address: ishwang@phys.sinica.edu.tw

some problems still exist in such algorithms. In this paper, we propose a postfitting control scheme for piezoelectric actuators. Compared with previous algorithms, this scheme demonstrates a high resolution, a high accuracy, and a fast response. It is especially suited for periodic motions, such as those in SPM scanning.

2. Postfitting Control Scheme

In the raster scanning of SPM, the *y*-scanner moves downward slowly, while the *x*-scanner makes a periodic left-and-right movement at a much faster speed. Therefore, we focus on the control of the *x*-scanner, with which it is more difficult to achieve both a high resolution and a high accuracy. The dynamics of the *x*-scanner can be identified using a second-order linear model coupled with the Bouc–Wen nonlinear model, as described below.

$$m\ddot{x} + c\dot{x} + kx = k(dv - h) \tag{1}$$

$$\dot{h} = \alpha d\dot{v} - \beta|\dot{v}|h - \gamma\dot{v}|h|, \tag{2}$$

where *h* indicates the hysteretic nonlinearity; α , β , and γ determine the magnitude and shape of the hysteretic loops; *v* is the input voltage; *d* is the piezoelectric coefficient; and *x*, *m*, *c*, and *k* represent the displacement, mass, damping, and stiffness of the *x*-scanner, respectively. This model can be numerically simulated using a Matlab/Simulink expression, as shown in Fig. 2.

We use a series of decaying triangular waves, as shown in Fig. 3(a), to drive a piezoelectric actuator (a piezoelectric stack element, PSt 150/5 × 5/20, Piezomechanik). The hysteresis behavior can be measured by an optical displacement sensor (a laser-based triangulation measurement system MICROTRAK 7000, MTI Instruments). The resolution of this sensor is ~100 nm with a bandwidth of 20 kHz. In Fig. 3(b), the gray line represents the measured trajectory and the black line represents the simulation result obtained using the above model. Both curves approximate each other, indicating the effectiveness of our mathematical model.

It is impossible to perfectly model a scanner’s behavior, because it is affected by many factors, such as piezoelectric nonlinearities, sample mass, the characteristics of electronic equipments, the crosstalk between axes, and the time-varying environment.²³⁾ Hence, a feedback strategy is needed to overcome these uncertainties. Figure 4(a) illus-

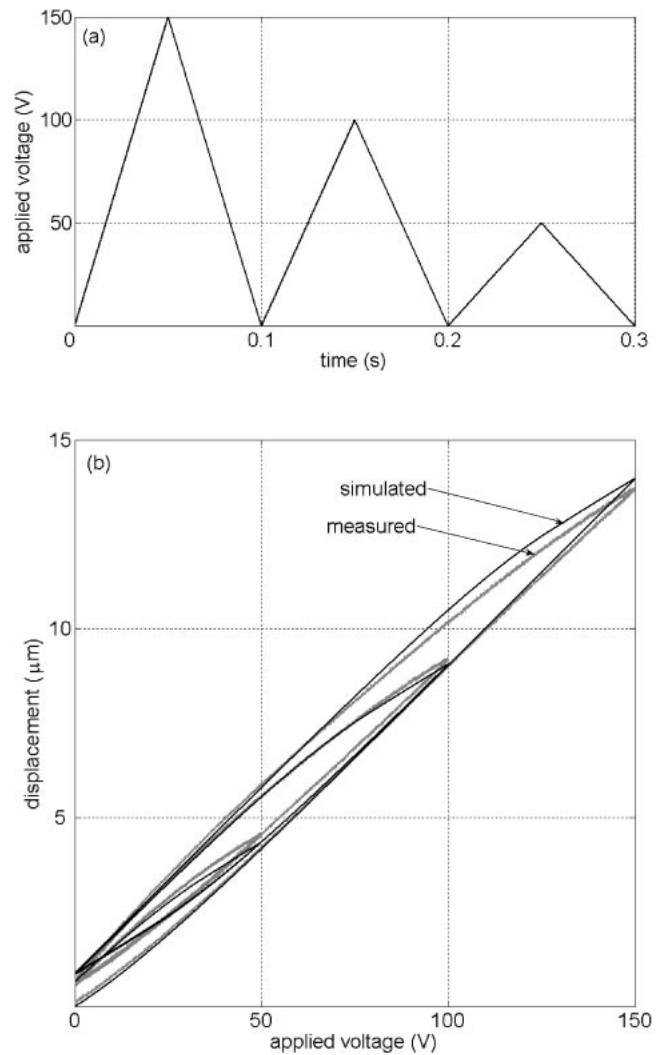


Fig. 3. (a) Series of decaying triangular waves used to drive piezoelectric actuator. (b) Hysteretic loops of piezoelectric actuator. The gray line indicates the measured trajectory by a displacement sensor and the black line represents the simulation results of *x* obtained from the Bouc–Wen model in Fig. 2.

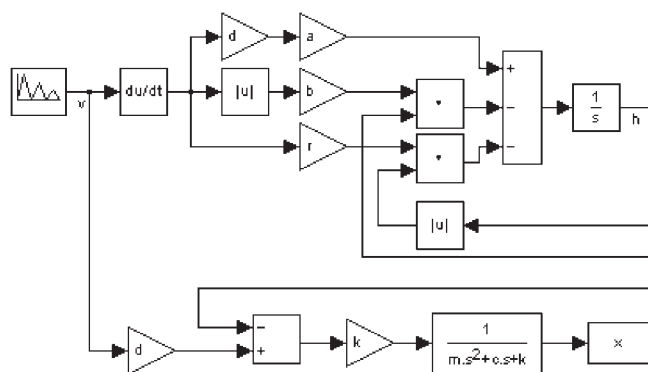


Fig. 2. Simulation diagram of piezoelectric actuator. The input *v* is a series of decaying triangular voltage signals shown in Fig. 3(a). The output *x* is the simulated displacement of the piezoelectric actuator. The simulation result is plotted in Fig. 3(b).

trates the experimental response of a low-gain feedback system, which has a poor tracking performance. We can increase feedback gains to improve tracking accuracy, but another problem may arise. The noise from the displacement sensor is amplified in the closed loop [see Fig. 4(b)], which often causes the oscillation of the scanner and degrades the resolution of the acquired SPM images, as demonstrated in Fig. 5(b). Therefore, the tradeoff between accuracy and resolution cannot be solved by pure feedback control.

There are two approaches to removing the high-frequency fluctuations. One approach is to add an on-line filter to suppress such fluctuations; however the filter also limits scanning speed. The other method is to perform an off-line smoothing on the driving signal, which is well suited for periodic scanning motions. Our proposed postfitting scheme is described below.

STEP 1: Prescanning. We adopt a high-gain PID control scheme to drive the *x*-scanner to track a specified ramping profile. In this prescanning, the *y*-scanner is held steady. Figure 4(b) shows that the measured motion basically follows the desired trajectory except for high frequency

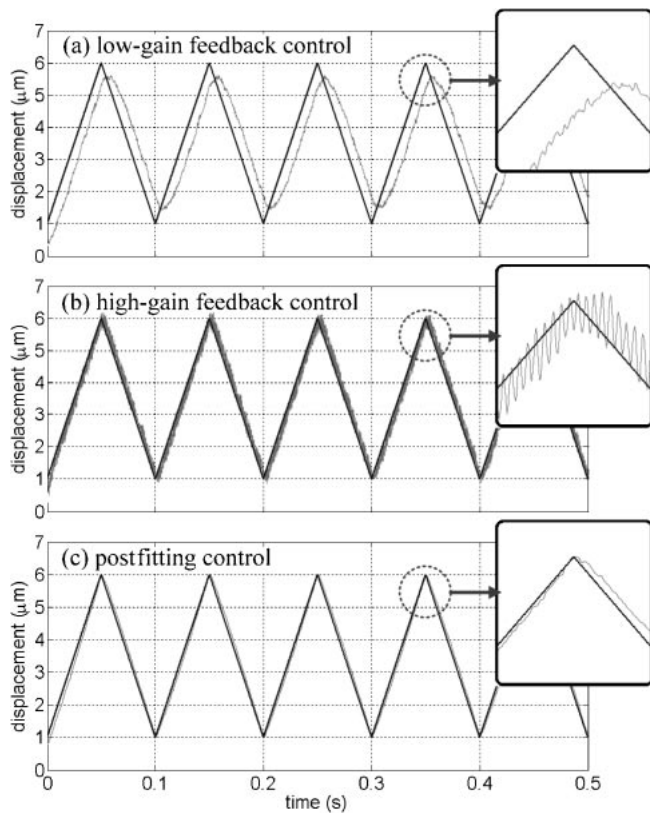


Fig. 4. Comparison of three different control schemes for x -scanning at the scanning speed of 10 line/s: (a) A poor tracking accuracy can be observed in the experiment with low-gain feedback control. (b) The tracking accuracy can be improved using high-gain feedback control, but resolution decreases due to the high-frequency noise. (c) Our postfitting control scheme demonstrates both on excellent tracking accuracy and a high resolution. In the figures, the black lines indicate the desired paths and the gray lines represent the measured paths.

fluctuations. This indicates that the feedback controller produces a good tracking signal for driving the scanner.

STEP 2: Fitting. We take the second to fifth cycles of the feedback controller's output signal and then average them. We do not use the first cycle because small deviations may occur in the initial several ms, as shown in Fig. 4(b). The averaged signal is still slightly noisy. It can be further

smoothened by curve-fitting methods. We carry out several polynomial fittings from the second-order to fifth-order, as shown in Fig. 6. We find that a fourth-order (as well as a fifth-order) polynomial provides a good fitting. As expected, a higher order fitting can achieve a smaller root-mean-square value of the fitting error. We adopt the fourth-order polynomial fitting because the fifth-order polynomial fitting does not show much improvement. In addition, two different polynomials are used to fit the left-to-right and right-to-left scanning motions.

STEP 3: Scanning. In this step, the displacement sensor is switched off. The fitting polynomial mentioned above takes the place of the feedback controller to drive the x -scanner in our image acquisition. A good tracking accuracy without high frequency noises is demonstrated in Fig. 4(c). Since this postfitting scheme needs no feedback control, it achieves both accuracy and resolution without sacrificing scanning speed.

3. Experimental Results

Our system is modified from a commercial atomic force microscope (AFM; A-100, AngsNanoTek) system. The scanner is a piezoelectric tube with multiple electrodes to generate three-axis motions. We add an aforementioned optical sensor to measure the displacement of the x -scanner. The scanning speed is 4 line/s. AFM images of a square grating (607-AFM, Ted Pella) taken with three different control schemes are shown in Fig. 5. Figure 5(a) shows a topographic image taken in the regular scanning mode, in which a saw-tooth waveform is applied to drive the x -scanner without any special control scheme. Even though the image resolution is good, the nonlinear distortion of the square grating in the x -direction is clearly observed. Figure 5(b) shows a topographic image taken with high-gain feedback control, in which information on the displacement sensor is fed back to a PID controller. The distortion in the square grating disappears, but the resolution decreases due to high-frequency noise in the driving signal of the x -scanner. Even if we decrease the gains of the PID controller, the resolution of the x -scanner is still limited by the measurement resolution of the displacement sensor, 100 nm. Figure 5(c) shows a well-resolved image with little

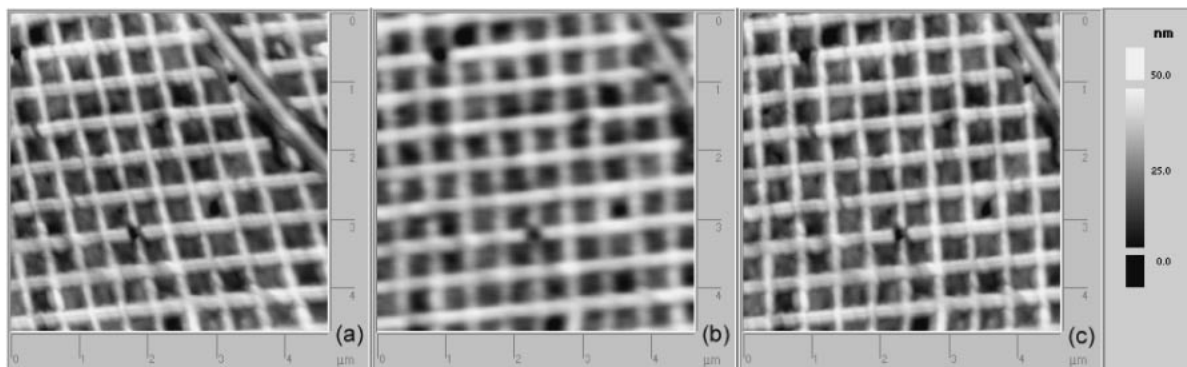


Fig. 5. Comparison of three different schemes in taking topographic images of square grating: (a) Image taken with regular AFM x -scan driven by saw-tooth signal. The squares on the right-hand side are more elongated in the x -direction than those on the left-hand side. (b) Image taken with high-gain feedback control. Although distortion in the x -direction is removed, fine features in the image are blurred due to high-frequency noise in the driving signal. (c) Image taken with postfitting control. The image shows little distortion in the square grating and a high resolution in the fine structures. Each image frame takes ~ 64 s to obtain.

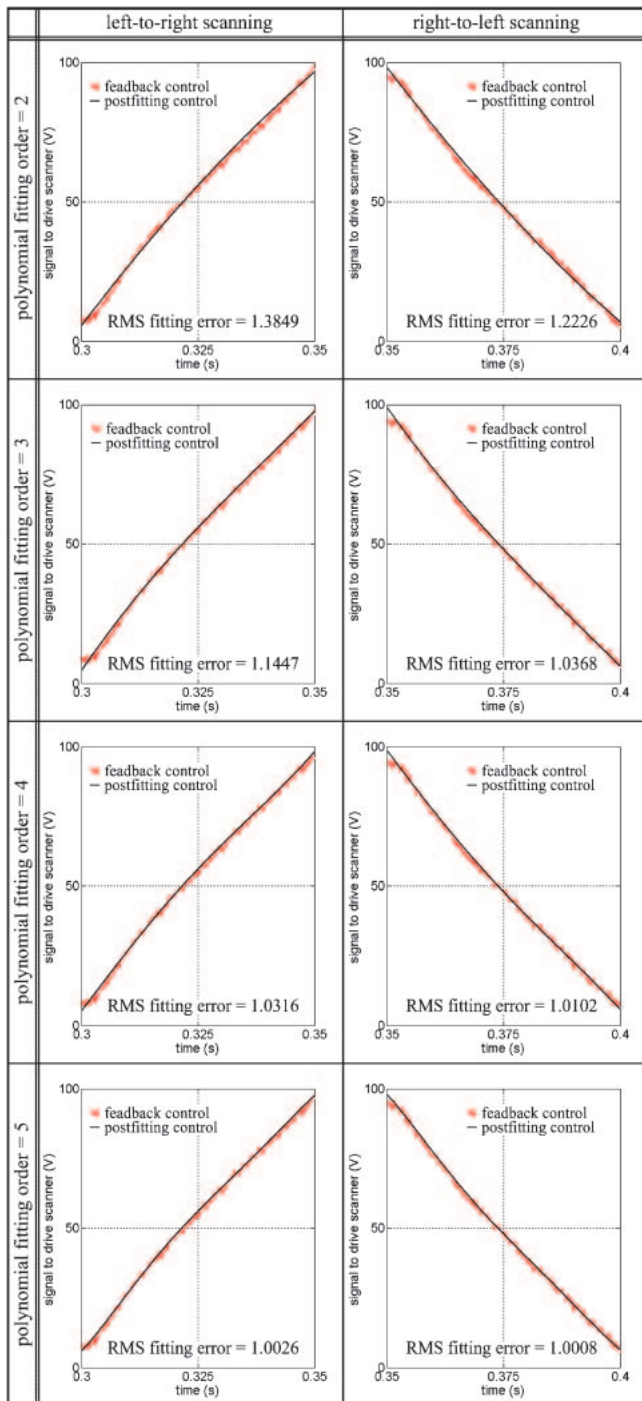


Fig. 6. Comparison of our fitting results from second-order to fifth-order polynomials. The left-to-right (shown in the left column) and right-to-left (shown in the right column) scanning directions are fitted separately with different polynomials. The oscillating red line shows the output of the feedback controller. The solid black line represents the fitting curve. It is clear that a higher order fitting can achieve a smaller fitting error.

distortion in the x -direction. This image is taken with the postfitting scheme described above. It takes only 1 s to perform the prescanning and fitting. Note that the fine structures of the grating can be clearly observed.

4. Discussions and Conclusions

Feedforward control uses information from system identification experiments to compensate the hysteresis of a piezoelectric scanner. However, the characteristics of a

scanner change with time. Thus, the performance of a feedforward controller degrades with time. Feedback control can overcome this time-varying problem by continuously sensing the displacement of the scanner. When it is applied to SPM, it is desirable that the sensor achieves nanometer resolution. Unfortunately, this kind of sensor usually responds slowly or has a high cost. If an inexpensive sensor is used, its noise may seriously limit the spatial resolution of an image.

Our proposed postfitting scheme integrates both the feedforward and feedback control schemes. In the prescanning, we utilize a feedback scheme to obtain a particular scan curve that can compensate the hysteresis and non-linearity of a piezoelectric scanner. Then, polynomial fitting preserves the unique shape of the curve but rejects high-frequency noise of the curve. During our image acquisition, the smoothed curve is used to drive the scanner without any feedback control.

Before each new image frame is taken, prescanning and curve fitting are carried out to compensate all time-varying factors. Therefore, the problems encountered in the feedforward as well as in the feedback control schemes do not appear in our new postfitting scheme. Note also that we do not use a very high resolution displacement sensor in our scheme.

In conclusion, we have developed a new method that combines both the closed-loop and open-loop methods and achieves distortion-free scanning without sacrificing spatial resolution or scanning speed.

Acknowledgment

The authors would like to thank Mr. Cherng-Ing Lin and AngsNanoTek Co. for valuable technical support. This research is supported by the National Science Council of ROC (contract #NSC93-2120-M-001-007) and Academia Sinica.

- 1) K. R. Koops, P. M. L. O. Scholte and W. L. de Koning: *Appl. Phys. A* **68** (1999) 691.
- 2) *Physik Instrumente: PI Catalog* (2004) 4-36.
- 3) P. Ge and M. Jouaneh: *IEEE Trans. Control Syst. Technol.* **4** (1996) 209.
- 4) P. Chen and S. Montgomery: *Ferroelectrics* **23** (1980) 199.
- 5) H. Jung, J. Y. Shim and D. G. Gweon: *Nanotechnology* **12** (2001) 14.
- 6) K. Takahashi, K. Tateishi, Y. Tomita and S. Ohsawa: *Jpn. J. Appl. Phys.* **43** (2004) 4801.
- 7) F. A. Garmon, W. T. Ang, P. K. Khosla and C. N. Riviere: *Proc. IEEE Int. Conf. Engineering in Medicine and Biology, Cancun, 2003, Vol. 4*, p. 17.
- 8) K. K. Leang and S. Devasia: *IEEE Int. Conf. Decision and Control, Hawaii, 2003, Vol. 3*, p. 2626.
- 9) E. Torre, J. Oti and G. Kadar: *IEEE Trans. Magn.* **26** (1990) 3052.
- 10) I. Mayergoyz, G. Friedman and C. Cailing: *IEEE Trans. Magn.* **25** (1989) 3925.
- 11) G. S. Choi, H. S. Kim and G. H. Choi: *Proc. IEEE Int. Symp. Industrial Electronics, Guimaraes, 1997, Vol. 3*, p. 851.
- 12) B. M. Chen, T. H. Lee, C. C. Hang, Y. Guo and S. Weerasooriya: *IEEE Trans. Control Syst. Technol.* **7** (1999) 160.
- 13) K. S. Narendra and K. Parthasarathy: *IEEE Trans. Neural Network* **1** (1990) 4.
- 14) M. Kawafuku, M. Sasaki and K. Takahashi: *Proc. IEEE/ASME Int. Conf. Advanced Intelligent Mechatronics, Atlanta, 1999*, p. 641.
- 15) M. Sasaki, M. Kawafuku and K. Takahashi: *Proc. IEEE Int. Conf. Neural Information Processing, Perth, 1999, Vol. 2*, p. 502.

- 16) C. J. Chien, L. C. Fu and A. C. Wu: *Automatica* **32** (1996) 833.
- 17) P. Krejci and K. Kuhnen: *IEE Proc. Control Theory Appl.* **148** (2001) 185.
- 18) K. Furutani, M. Urushibata and N. Mohri: *Proc. IEEE Int. Conf. Robotics and Automation, Leuven, 1998, Vol. 2, p. 1504.*
- 19) S. H. Hsu and L. C. Fu: *Proc. IEEE Int. Conf. Control Applications, Hawaii, 1999, Vol. 2, p. 1626.*
- 20) *Physik Instrumente: PI Catalog (2004) 2-40.*
- 21) T. Chang and X. Sun: *IEEE Trans. Control Syst. Technol.* **9** (2001) 69.
- 22) G. Schitter, F. Allgower and A. Stemmer: *Nanotechnology* **15** (2004) 108.
- 23) H. Kawai: *Jpn. J. Appl. Phys.* **8** (1969) 975.